Available online at www.sciencedirect.com
SCIENCE DIRECT®
Applied Radiation and Isotopes 62 (2005) 681–692
Applied Radiation and Isotopes
www.elsevier.com/locate/apradiso

Simulation of corrosion product activity for nonlinearly rising corrosion on inner surfaces of primary coolant pipes of a typical PWR under flow rate transients

Nasir M. Mirza[a,*], Muhammad Rafique[a], Sikander M. Mirza[a], M. Javed Hyder[b]

[a]*Department of Physics & Applied Mathematics, Pakistan Institute of Engineering & Applied Sciences, Nilore, Islamabad 45650, Pakistan*
[b]*Department of Mechanical Engineering, Pakistan Institute of Engineering & Applied Sciences, Nilore, Islamabad 45650, Pakistan*

Received in revised form 5 November 2004; accepted 5 December 2004

Abstract

For nonlinear accelerating corrosion, calculation of activated corrosion products on inner surfaces of primary coolant pipes have been done in a typical pressurized water reactor (PWR) under flow rate perturbations. Computer program CPAIR-P (Corrosion Product Activity In Reactors) (Deeba et al., 1999) has been modified to accommodate for time-dependent corrosion rates. Results, for ^{24}Na, ^{56}Mn, ^{59}Fe, ^{58}Co, ^{60}Co and ^{99}Mo, show that the specific activity in primary loop approaches equilibrium value under normal operating conditions fairly rapidly. Predominant corrosion product activity during operation is due to ^{56}Mn, and cobalt isotopes dominate the activity after shutdown of reactor. Flow rate perturbations and different types of rising corrosion rates were introduced in the system and effects on saturation activity were studied. For a linear decrease in flow rate and a constant corrosion rate, the total coolant activity and activity on pipe scale approaches higher saturation values when compared to normal condition values. With a nonlinearly accelerating corrosion, the behavior of specific activity changes considerably. The flow rate perturbations on specific activity for pipe scale results in a new saturation value which depends on both the changes in flow rate (Δw) and equilibrium corrosion rate (C_s) values. However, the time taken to reach the saturation activity depends on the slope of corrosion rate. For a slow pump coastdown, the activity does not show an initial drop when flow rate starts decreasing. It monotonically rises and follows the slope of corrosion rate. The peak value and decay of activity after scram are strong functions of flow rate and removal efficiencies.

Keywords: Computer modeling and simulation; Corrosion products; Flow rate transients in pressurized water reactors (PWRs); Corrosion rate

1. Introduction

The pressurized water reactors (PWRs), which comprise more than two third majority of operating power reactors worldwide, have one to two orders of magnitude higher steam generator dose rates as compared with the gas- or sodium-cooled reactors. This results in prolongation and reduced effectiveness of reactor maintenance and translates into estimated penalties of the order of several million dollars per unit annually (Moore, 1984). These high dose rates in the primary circuits of PWRs are essentially due to the coolant as well as the corrosion product activation, and out of these two, the later is recognized as the dominant

*Corresponding author. Tel.: +92 51 9290273; fax: +92 51 9223727.
E-mail address: nasirmm@yahoo.com (N.M. Mirza).

0969-8043/$ - see front matter © 2005 Elsevier Ltd. All rights reserved.
doi:10.1016/j.apradiso.2004.12.005

factor in the prolongation of necessary plant maintenance (Comley, 1985; Lister et al., 1985; Cohen, 1969). The corrosion in PWRs occurs due to liquid–metal interaction and dominant constituents of the cladding and piping metals are released into the coolant as corrosion products which may be in particulate form or in dissolved state. Since steel and inconel are common structural materials used in PWRs, the corrosion products mainly contain iron, nickel, chromium and cobalt. These corrosion products become activated as they pass through the core region, and in the primary loop they may be deposited at various places. Later, these may be released again in the turbulent flow of coolant. The coolant activity is therefore dependent on the rate of corrosion, deposition and re-release of the particulate corrosion products.

Due to its importance, a lot of research effort has been directed towards the estimation of the corrosion product activity in reactor coolants in past. Detailed studies on deposition of such particles in turbulent flows were carried out (Beal, 1970). Cleaver and Yates (1973) carried out studies for colloidal particle detachment in turbulent flows. Later, they developed a sub-layer model for the deposition of such particles from turbulent flows (Cleaver and Yates, 1975). Lister (1976) studied the mass transfer phenomenon for steel isothermal surfaces. Then, Berger and Hau (1977) carried out experimental measurements of mass transfer in turbulent pipe flows. Beslu (1978) developed the computer program PACTOLE for predicting the time-dependant behavior of the activation of corrosion products in PWRs. Using this code it was found that temperature is the main driving force in corrosion product transport and buildup, while water chemistry also plays an important role (Beslu, 1981). The coolant chemistry has been identified as playing the most important role in the buildup of radiation field in PWRs (Bergmann and Lindsay, 1985). Based on the more recent experimental data, CORA code was upgraded to model the transport of corrosion products in primary loops of PWRs (Kang and Sejvar, 1985). Studies were also directed towards the buildup of corrosion products in LWR fuel rods (Strasser et al., 1985). Work was done to estimate the mass of various corrosion products in Westinghouse PWRs (Polley and Pick, 1986). Models were developed for the study of radionuclide transport in simpulated PWR environment (Morillon, 1987). Efforts were also made for detailed analytical model development for the calculation of thermodynamic as well as the transport properties of aqueous species in high-pressure and high-temperature environment of PWRs (Oelkers and Helgeson, 1988). In-pile loops have been used for the experimental study of possible improvements in the coolant chemistry for reducing the corrosion product dose rates (Sanchez, 1989; Lee, 1990). These studies indicate that dissolution and crystallization cannot be modeled accurately enough in the absence of the required experimental coefficients for these processes.

In modern times, the severity of corrosion product activity problem is further aggravated by the fact that with the advent of higher power fuel, the potential for additional crud deposition on core has increased (Millett and Wood, 1997). Reportedly, several plants operating with localized boiling in some parts of the core have experienced an axial offset anomaly (AOA), which has been attributed to concentration of lithium boron compounds in crud deposits. In recent studies also, for steam cycles, corrosion cracking, such as stress corrosion and corrosion fatigue, pitting, erosion-corrosion (flow-accelerated corrosion), and localized fast general corrosion (usually in boiler tubes) due to concentrated salts, acids, or sodium hydroxide have been identified as the biggest concern (Jonas, 2000).

Detailed studies have revealed that the rate of corrosion in the reactor primary system keeps on increasing as the time of reactor operation at full power increases. Such acceleration in corrosion is a nonlinear function of time with plant aging. Access and frequent maintenance to areas near primary pumps becomes very limited due to high radiation doses from primary water and pipe scale (Dey et al., 1998; Hirschberg et al., 1999; Varga et al., 2001).

During normal operation of PWRs, the corrosion product activity is primarily due to short-lived ^{56}Mn and ^{24}Na. Nearly all the long-lived activity in the coolant is due to iron, molybdenum and cobalt with most significant radionuclides as ^{59}Fe, ^{99}Mo, ^{58}Co and ^{60}Co. Various nuclear properties of these nuclides are shown in Table 1 (Jaeger, 1970). The ^{55}Mn has an activation cross-section of 13.4 b for the thermal neutrons to produce ^{56}Mn. The neutron activation of structural ^{27}Al and activation of ^{23}Na from salt impurities in water can produce ^{24}Na. The use of high-purity water, demineralization of water and the presence of filters keep the amount of dissolved salts to less than 0.05 ppm (Jaeger, 1970). It was seen for low-powered nuclear plants, having large aluminum fraction in the system, the coolant activity due to ^{24}Na remained comparable to ^{16}N activity (Mirza et al., 1989, 1991). It was also shown in subsequent experimental studies that the effect of sodium salt as an impurity in coolant remains small as compared to ^{24}Na resulting from aluminum activation (Mirza et al., 1997a). However, the half lives of all corrosion products remains for more than 2 h. Therefore, the primary coolant will always retain activity for several hours even after the reactor shutdown and any transient condition during operation can further increase the coolant activity.

The turbulent flow of coolant in primary coolant loop keeps on depositing activated nuclides as it passes through the flow channels of the primary coolant loop. These deposits of dissolved and suspended radionuclides

Table 1
Activation products and their reaction properties

Corrosion products	Reaction and neutron energy	Activation cross-section and half-life	γ-ray energy
^{24}Na	^{27}Al(n, α)^{24}Na	6×10^{-4} b	4.1 MeV
	($E_n > 11.6$ MeV)	(15.4 h)	
	^{23}Na(n, γ)^{24}Na	0.53 b	
	(E_n is thermal)	(15.4 h)	
^{56}Mn	^{55}Mn(n, γ)^{56}Mn	13.4 b	2.13 MeV (15%)
	(E_n is thermal)	(2.58 h)	1.81 MeV (24%)
^{59}Fe	^{58}Fe(n, γ)^{59}Fe	0.9 b	1.17 MeV (99.9%)
	(E_n is thermal)	(45.1 h)	1.33 MeV (99.9%)
^{58}Co	^{58}Ni(n, p) ^{58}Co	0.146 b	—
	(E_n is fast)	(70.88 days)	
^{60}Co	^{59}Co(n, γ) ^{60}Co	20 b (5.3 years)	1.173 MeV (99.9%)
			1.332 MeV (99.9%)
^{99}Mo	^{98}Mo(n, γ) ^{99}Mo	0.45 b (67.0 h)	0.78 MeV (8%)
	($E_n > 3.1$ MeV)		0.74 MeV (8%)

on the scale of primary circuit's inner surfaces do pose maintenance issues. Chemical procedures to find amounts of corrosion products in primary coolants of PWRs after shutdown were studied by Raymond and his colleagues for both target and active nuclides. They showed that detection limits are between 0.05 and 0.3 mg/L for undissolved species and for ions these are in the range of 0.03–0.14 mg/L for sample volumes of 0.5 L (Raymond et al., 1987). Recently, Hirschberg and his colleagues have also experimentally studied accumulation of radioactive corrosion products on steel surfaces of VVER-type nuclear reactors for ^{60}Co buildup on steel surfaces (Hirschberg et al., 1999; Varga et al., 2001). Effects of corrosion inhibitors, on corrosion rates for carbon steel, were also studied by Dey et al. (1998) and they proposed high-efficiency organic inhibitors for base metal protection.

Operating parameters of the reactor also affect strongly the types of radionuclides formed, the levels of saturation activity reached and the rates at which the saturation is reached. These include the composition of the materials in contact with the coolant, amount and the types of the impurities present in the coolant, reactor power, residence time of coolant in core, temperatures and pressure, coolant flow rates, corrosion rates, filter efficiency and deposition rates of radioactive elements. During the past decade, many studies were conducted on coolant activation with specific interest to find effects of flow rate and power perturbation on dose rate in medium-flux research reactors (Mirza et al., 1989, 1991). Calculations of coolant activation were also done for low-flux natural convection-based systems (Mirza et al., 1993a, b). Experimental measurements of ^{24}Na activity in low-power research reactors yielded that majority of ^{24}Na comes from neutron activation of ^{27}Al and its subsequent mixing in coolant, and it is the second important contributor to the total dose after ^{16}N in coolant activity. (Mirza et al., 1997a). It was seen in simulations of both low- and high-flux systems that transients under reactivity and loss of flow do lead to peaking of neutron flux in reactor and production of high activity in coolant (Iqbal et al., 1996, 1998; Mirza et al., 1998). These strongly affect the coolant activity and corrosion rate. Sensitivity analysis of reactivity insertion limits with respect to safety parameters in typical MTRs showed that neutron flux peaking and clad melting conditions are dictated by void coefficients, transient type and their rates (Nasir et al., 1999). Void coefficient, Doppler coefficient and temperature of moderator showed significant effects on power peaking in a non-uniform manner within the core. It also led to the necessity of performing detailed space and time calculations of flux for conditions (Khan et al., 1999).

Modeling of corrosion products activity in primary coolants of PWRs under flow rate perturbations were also done to investigate effects due to flow coastdown (Mirza et al., 1997b). A computer code CPAIR (Corrosion Product Activity In Reactors)was developed in FORTRAN-77 to calculate specific activity due to corrosion products in primary water of light-water reactors. It was shown that minimum value of coolant activity depends strongly on the slope of linear decrement of flow rate. The program was further improved to incorporate the effect of power perturbations on corrosion product activity in coolants of a PWR (Deeba et al., 1999). The computer code was modified as CPAIR-P and effects of fast and slow transients were studied on dose rates due to corrosion activity in coolant. All these studies assumed a constant and uniform corrosion rate during and after transients. However, the corrosion rate does increase slowly with plant operating at full power; it also increases with

temperature and pressure. The rate of increase of corrosion depends on integrated effect of neutron flux, time of reactor operation and reactor temperatures (Fontanna, 1987; Glasstone & Sesonske, 1981).

For nonlinearly rising corrosion, method and calculations of corrosion product activity on inner surfaces of primary coolant piping are presented in this work. These are furthermore superimposed on flow rate perturbations to study their influence on the total activity in primary circuit. The computer program CPAIR-P (Mirza et al., 1998, Deeba, et al., 1999) was modified to incorporate both the accelerating corrosion and flow rate perturbations. Calculations for specific activity due to ^{24}Na, ^{56}Mn, ^{59}Fe, ^{58}Co and ^{99}Mo in the coolant and on primary pipe scale have been done. First, we compared the total activity for a uniform and fixed corrosion rate under different flow rate transients in a PWR. Then, both accelerating corrosion rates and different types of flow rate perturbations were introduced and the behavior of corrosion product activity on primary pipe scale was studied. Results for fast and slow corrosion acceleration and flow rate perturbations are presented here.

2. Mathematical model

The concentration of target nuclides in the primary coolant water, on the inner walls of the piping and on the core surfaces have been denoted by N_w, N_p and N_c, respectively, in atoms/cm^3. Also the concentrations of the activated nuclides in primary water, on the piping and on the core have been represented by n_w, n_p and n_c, respectively, in atoms/cm^3. Possible paths leading to various productions and losses of corrosion products are shown in Fig. 1. Then the rate of change of active material concentration in primary coolant is (Mirza et al., 1997b; Deeba, et al., 1999)

$$\frac{dn_w}{dt} = \sigma\phi_\varepsilon N_w - \left\{\sum_j \frac{\varepsilon_j Q_j g(t)}{V_w} + \sum_k \frac{l_k g(t)}{V_w} + \lambda\right\} n_w + \frac{K_p g(t)}{V_w} n_p + \frac{K_c g(t)}{V_w} n_c, \quad (1)$$

where, σ is the group constant for the production of isotope from target nuclide; ϕ_ε is the effective group flux (neutrons/cm^2 s); N_w is the target nuclide concentration

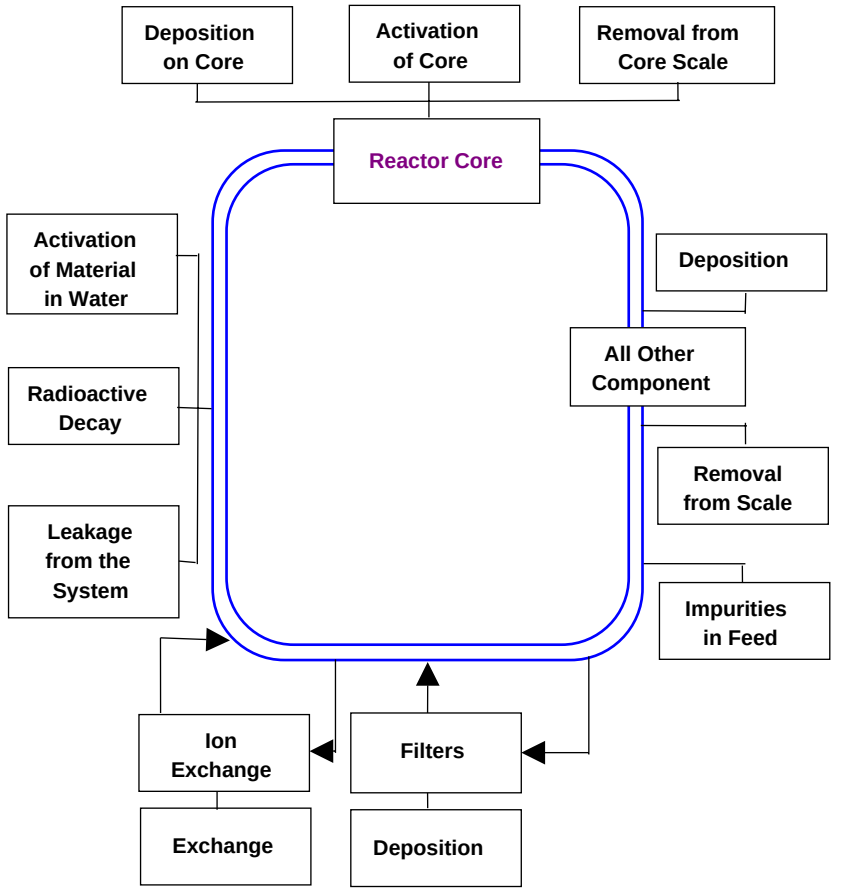

Fig. 1. Production and loss paths for corrosion products in primary coolant circuit of a typical PWR.

Table 2
Experimental values of exchange rates in a typical PWR[a]

Rate type	Value
Deposition on core ($\varepsilon_c Q_c$) (cm^3/s)	80.0
Deposition on piping ($\varepsilon_p Q_p$) (cm^3/s)	13.7
Ion-exchanger removal ($\varepsilon_I Q_I$) (cm^3/s)	500–781
Re-solution ratio for core (K_c) (cm^3/s)	40.0
Re-solution ratio for piping (K_p) (cm^3/s)	6.9
Volume of primary coolant (V_w) (cm^3)	1.37×10^7
Volume of scale on core (V_c) (cm^3)	9.08×10^6
Volume of scale on piping (V_p) (cm^3)	1.37×10^6
Total corrosion surface (S) (cm^2)	1.01×10^8

[a]References: Jaeger (1970), Glasstone and Sesonske (1981).

in water (atoms/cm^3). The sum over j for $\varepsilon_j Q_j$ is given as following:

$$\sum_j \varepsilon_j Q_j = \varepsilon_I Q_I + \varepsilon_p Q_p + \varepsilon_c Q_c + \varepsilon_F Q_F, \tag{2}$$

where the quantities $\varepsilon_I Q_I$, $\varepsilon_p Q_p$, $\varepsilon_c Q_c$ and $\varepsilon_F Q_F$ are removal rates due to ion exchanger, deposition on pipes, deposition on core surfaces and removal by filters, respectively. The term l_k is the rate at which primary coolant loop loses water from its k'th leak (cm^3/s); K_p and K_c are rates at which isotopes are removed from the scale on piping (cm^3/s) and from the core (cm^3/s), respectively. For a typical PWR the measured values of these removal rates are shown in Table 2. The first term on left-hand side of Eq. (1), represents the production of radioactive isotopes. The second term is the rate at which the active nuclides are lost as a result of purification by the ion-exchanger and filters, deposition on the piping and core, and decay. The third and fourth terms are the rates at which the activity is re-introduced into the coolant by erosion from scale on piping and the core. To include any flow rate perturbation we define a parameter $g(t)$:

$$g(t) = w(t)/w_0, \tag{3}$$

where w_0 is the steady-state flow rate under normal operations and $w(t)$ is the time-dependent flow rate. The values of decay constant (λ) for isotopes of interest are provided in Table 1. The group flux ϕ_0 is averaged over the geometry of the core and have been estimated using programs LEOPARD (Barry, 1963) and ODMUG (Thomas and Edlund, 1980) in the code CPAIR-P as subroutines. The time T_c and T_L are the core residence time and loop time (required to complete the primary loop once), respectively. The core residence time is

$$T_c = \frac{H\rho A}{w(t)}, \tag{4}$$

where H is the core height, A is the flow cross-sectional area in cm^2, ρ is the coolant density at operating temperatures and $w(t)$ is the time-dependent flow rate (g per second). The loop time is calculated as $V_w T_c/(HA)$, where V_w is the coolant volume in primary loop.

The rate of buildup of target nuclide concentration in coolant water can be written as

$$\frac{dN_w}{dt} = -\left\{\sum_j \frac{\varepsilon_j Q_j g(t)}{V_w} + \sum_k \frac{l_k g(t)}{V_w} + \sigma\phi_\varepsilon\right\} N_w + \frac{K_p g(t)}{V_w} N_p + \frac{K_c g(t)}{V_w} N_c + S_w, \tag{5a}$$

$$S_w = \frac{C(t)S}{V_w}\frac{N_0}{A} f_n f_s, \tag{5b}$$

where N_p is concentration of target nuclide on the piping, N_c is concentration of target on the core and S_w is the source term for corrosion. The $C(t)$ is the time-dependent corrosion rate (g/cm^2 s), S is the area of system exposed to coolant for corrosion; N_0 is Avogadro's number (6.023×10^{23} atoms/g mol) and A is the atomic weight of the target nuclide (g). Here, f_n and f_s are abundances of target nuclide and chemical element in the system, respectively.

The impurity removal by ion-exchanger, core deposition and leakage are directly related to the flow rate. Also, the rate of re-entry from scales is directly proportional to the primary coolant flow rate. Therefore, the rate of activity buildup on the core scale is given by

$$\frac{dn_c}{dt} = \sigma\phi_0 N_c + \frac{\varepsilon_c Q_c g(t)}{V_c} n_w - \left\{\frac{K_c g(t)}{V_c} + \lambda\right\} n_c, \tag{6}$$

where V_c is the volume of the scale on the core(cm^3) and ϕ_0 is thermal neutron flux average over the geometry of the core (neutrons/cm^2 s).

The rate of buildup of target nuclide concentration on the core scale (N_c) is given by the following equation:

$$\frac{dN_c}{dt} = \frac{\varepsilon_c Q_c g(t)}{V_c} N_w - \left\{\frac{K_c g(t)}{V_c} + \sigma\phi_0\right\} N_c. \tag{7}$$

The rate of deposition of active material on the piping scaling (n_p) can be obtained from following balance:

$$\frac{dn_p}{dt} = \frac{\varepsilon_p Q_p g(t)}{V_p} n_w - \left\{\frac{K_p g(t)}{V_p} + \lambda\right\} n_p, \tag{8}$$

where V_p is the volume of scale on the piping (cm^3). Then the rate of change of target nuclide on piping walls (N_p) is

$$\frac{dN_p}{dt} = \frac{\varepsilon_p Q_p g(t)}{V_p} N_w - \frac{K_p g(t)}{V_p} N_p. \tag{9}$$

Based on the above system of Eqs. (1)–(9), the computer program CPAIR-P (Deeba et al., 1999) was modified for this work to include the effect of both accelerating corrosion rate and flow rate perturbations as a function of time. The modified CPAIR-P program

Table 3
Typical design specifications of a PWR

Parameter	Value
Specific power (MW(th)/kg U)	33
Power density (MW(th)/m^3)	102
Core height (m)	4.17
Core diameter (m)	3.37
Assemblies	194
Rods per assembly	264
Fuel type	UO_2
Clad type	Zircoloy
Lattice pitch (mm)	12.6
Fuel rod outer diameter (mm)	9.5
Average enrichment (w%)	3.0
Flow rate (Mg/s)	18.3
Linear heat rate (kW/m^2)	17.5
Coolant pressure(MPa)	15.5
Inlet coolant temperature (°C)	293
Outlet coolant temperature (°C)	329

is written in FORTRAN-77 for Personal Computers. After initialization, it calculates group constants using core design parameters (Table 3) in LEOPARD (Barry, 1963) program. The LEOPARD program is a zero-dimensional unit cell computer code with 54 fast and 172 thermal energy groups. Evaluated nuclear data (ENDF-IV) set has been used in the cross-section library. In this work, equivalent cells of a typical PWR (Glasstone and Sesonske, 1981) have been employed to generate group constants for fuel cells and water holes. These cell-averaged group constants are then used in the one-dimensional multigroup diffusion theory-based ODMUG (Thomas and Edlund, 1980) code. The ODMUG calculates the group fluxes as a function of position in the reactor. These group fluxes are subsequently averaged over the core. Both LEOPARD and ODMUG are treated as subroutines of the CPAIR-P program. Then Eqs. (1)–(9) are solved using fourth-order Runge–Kutta method to find the activity values due to corrosion products in primary coolant, on piping, and on core surface.

3. Simulation results

For a typical 1000 MWe pressurized water reactor (Glasstone and Sesonske, 1981) with initial impurity concentrations taken to be zero has been considered in this analysis. The design parameters for the system are given in Table 3 (Glasstone and Sesonske, 1981). The fractional exchange rates ($\varepsilon_j Q_j / V_q$) and re-solution rates K_j / V_q employed in the calculations are shown in Table 2 (Jaeger, 1970). The core averaged group fluxes have been computed using LEOPARD and ODMUG codes for the system. The plant surface area of about $10^8\,cm^2$ is exposed to the primary coolant for corrosion and in the presence of corrosion inhibitors, an equilibrium corrosion rate density of $2.4\times10^{-13}\,g/cm^2\,s$ (Jaeger, 1970; Glasstone and Sesonske, 1981) exists after a year of reactor operation. It has corrosion rate of 25 μg/s and primary coolant volume of $1.3\times10^7\,cm^3$.

The purification rate due to an ion-exchanger, $\varepsilon_I Q_I$, must be large enough to regard deposition, re-solution and leakage as second-order effects. Therefore, using an approach by Mirza et al. (1997a) an optimum removal rate of activity by the ion-exchanger was determined at a constant corrosion rate. It was found that saturation value of coolant activity remains fixed when $\varepsilon_I Q_I$ is more than $400\,cm^3/s$. Thus a conservative removal rate of $600\,cm^3/s$ was selected for which the saturation value of activity is sufficiently low.

Six corrosion products (^{56}Mn, ^{24}Na, ^{59}Fe, ^{60}Co, ^{58}Co and ^{99}Mo) were considered in this study. Specific activities in primary coolant, on inner surfaces of pipes and on core surface, as a function of reactor operation time are shown in Fig. 2 for ^{60}Co, ^{58}Co, ^{56}Mn and ^{24}Na. When a system has constant corrosion rate and reactor is in operation at full power, the isotope ^{56}Mn remains the largest contributor to the total activity (Fig. 2). Its activity in primary coolant during operation is about 36% of the total corrosion product activity in the PWR whereas other isotopes including ^{24}Na, ^{59}Fe, ^{99}Mo and ^{60}Co contribute about 23.4%, 29.6%, 9.5% and 1.4%, respectively. The activity due to ^{56}Mn saturates within 200 h of reactor operation at full power. The saturation values in the coolant, on pipe scale and on core scale are 15.87, 2.09 and 56.43 μCi/cm^3, respectively. In this study, the system was allowed to shut down at $t=$ 1000 h. The activity on core surface and pipes due to cobalt remains high after shutdown (Fig. 2). The total activity due to all corrosion products as a function of time is given in Fig. 3. During operation, the highest contributor to activity is scale on core surface and the second largest part comes from primary pipe scale. When rector is shut down, the total activity due to pipe scale becomes the largest source and it decays slowly due to contributions of cobalt (Figs. 2 and 3). Saturation activity values for primary coolant, on pipe scale and on core surface are 17.3, 12.9 and 74.1 μCi/cm^3, respectively. These are close to already reported values by Mandler et al. (1985) and Volleque (1990) in their source term measurements.

3.1. Constant corrosion rate and flow rate perturbations

Flow rate perturbations in a PWR can occur due to some variation in the cross-sectional area of the flow channels or due to changes in primary pump speed.

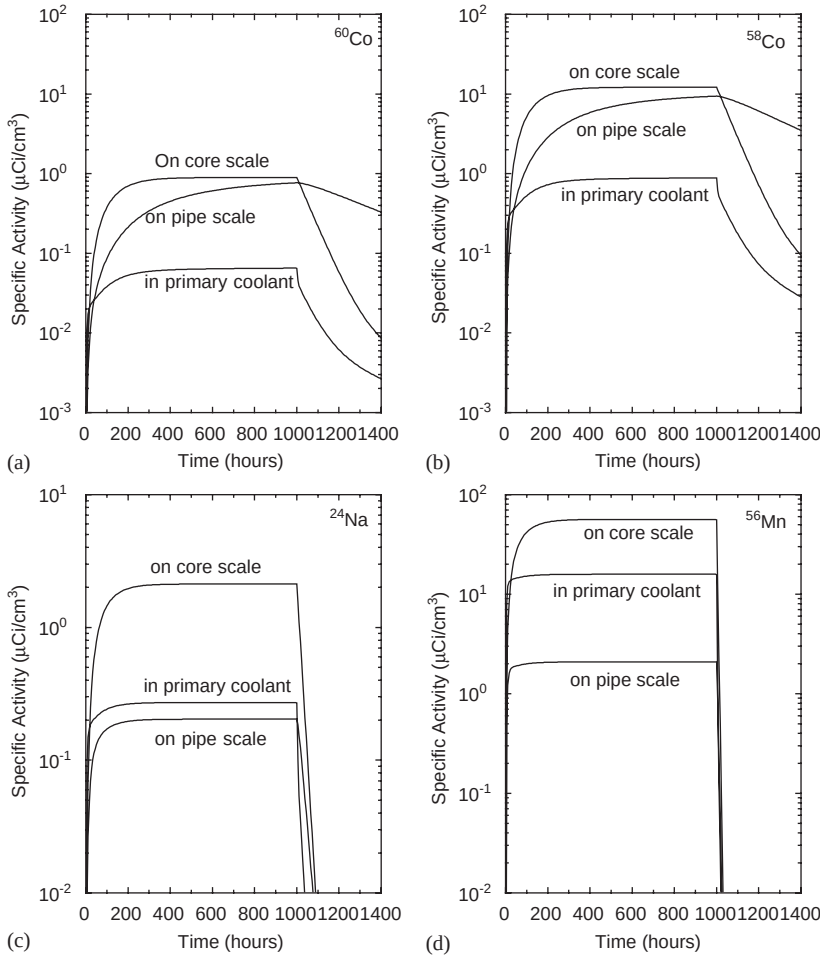

Fig. 2. Specific activity for ^{60}Co(a), ^{58}Co(b), ^{24}Na(c) and ^{56}Mn(d) in primary coolant, on inner surfaces of pipes and on core surfaces as a function of reactor operation time under normal conditions and constant corrosion rate. System shuts down at $t = 1000$ h.

These perturbations subsequently affect temperatures, neutron flux in the core, corrosion production terms and loss terms. The load-following system then tries to adjust the flow rates in the reactor; however, if it cannot do so then the reactor scrams. In this work, flow perturbations are introduced during the steady-state operation of the reactor when corrosion product activity has reached its saturation value. Then corrosion product activity in coolant and pipe scale is observed using the CPAIR-P program.

A linear decrease in flow rate is introduced (at $t = 500$ h) for the reactor operating at full power under steady-state conditions. Corrosion products have reached saturation values. The reactor normally undergoes a scram at low flow rate condition. Since we are interested in studying the transient response of corrosion product activity even in this state, the reactor is not allowed to undergo a scram during the transient. This decrease in the flow can be described by a parameter $g(t)$:

$$g(t) = \begin{cases} 1, & t < t_{\text{in}}, \\ 1 - \alpha(t_{\text{in}} - t), & t_{\text{in}} < t < t_{\text{in}} + \Delta t, \\ w_2/w_0, & t > t_{\text{in}} + \Delta t, \end{cases} \tag{10}$$

where α is the slope of flow rate decrement and t_{in} is the time at which the disturbance in the mass flow rate is initiated. After time $t_{\text{in}}+\Delta t$, the flow rate achieves a lower value w_2 as compared to w_0. Such a flow rate change affects T_{c} and T_{L}, causing a change in the production rate of corrosion product activity.

In the first part of the study, the above parameter, $g(t)$, is introduced as a perturbation while the corrosion rate is kept constant. The flow rate is introduced at $t_0 = 500$ h for various Δw changes for a period $\Delta t = 100$ h. Both the total specific activity in coolant and on the pipe scale in the

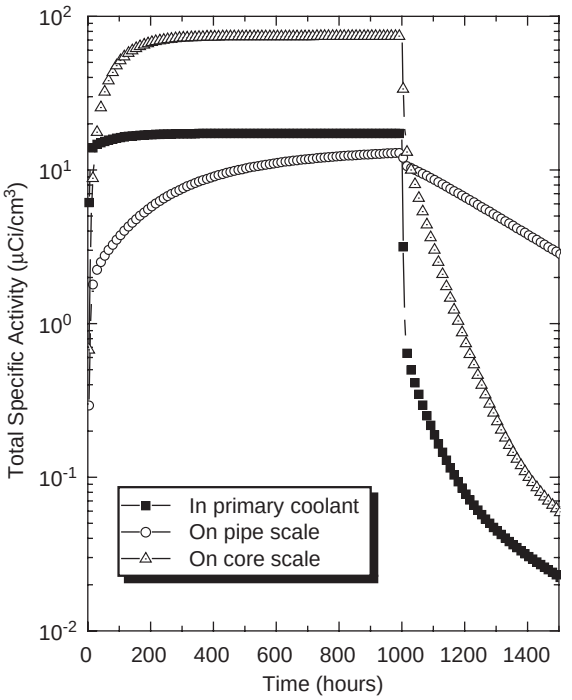

Fig. 3. Comparison of total specific activity due to corrosion products in primary coolant, on surfaces of pipes and core as a function of reactor operation time at full power under normal conditions and constant corrosion rate.

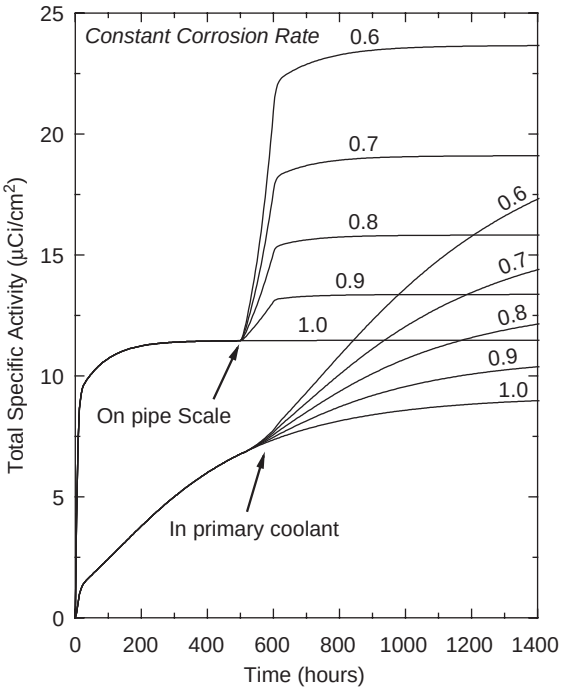

Fig. 4. Total specific activity due to corrosion products in primary coolant and on primary pipe scale of a PWR under linear flow rate perturbation for various Δw (initiated at $t = 500$ h, $\Delta t = 100$ h). The corrosion rate is assumed to be constant and uniform.

presence of a flow rate perturbation are shown in Fig. 4. As the flow rate decrease to 10% of its rated value, both activities attain new saturation values (about 17% higher as shown in Fig. 4). For coolant activity, the new saturation value is 66% higher when we test the plant for a decrease of 30% in the flow rate. The activity due to pipe scale rises slowly. When the flow rate transient is introduced at $t = 500$ h, the resultant activity on pipe scale attains new saturation values for different flow changes (Δw) as shown in Fig. 4. For a 10% decrease in flow rate, the saturation value of activity on pipe scale increases from 9.1 to 10.7 μCi/cm^3. When we allowed the flow rate to decrease to $0.6w_0$, we notice an increase of more than 80% in the saturation activity. Such a hike in source will result in even larger doses outside primary circuit near pump and heat exchanger.

3.2. Nonlinear acceleration of corrosion

Slow and fast acceleration have been studied using following model for time-dependent corrosion rate $C(t)$:

$$C(t) = \begin{cases} 0, & t < t_{\text{in}}, \\ C_{\text{s}}[1 - \exp(-M_{\text{c}}(t - t_{\text{in}}))], & t_{\text{in}} < t < t_{\text{in}} + \Delta t, \\ C_{\text{s}}, & t > t_{\text{in}} + \Delta t, \end{cases} \tag{11}$$

where M_{c} is a non-zero positive constant slope of corrosion rate in the time domain $[t_{\text{in}}, t_{\text{in}} + \Delta t]$ and C_{s} is the equilibrium value of the rate after time $t_{\text{in}} + \Delta t$. A corrosion-free time period, t_{in}, about 50 h after the startup is assumed. We introduce such a time-dependent corrosion rate along with a flow rate perturbation as shown in Fig. 5a. As a first step, we used a constant equilibrium value (25 μg/s) and allowed changes in M_{c}. The resultant specific activity due to all corrosion products on pipe scale is given in Fig. 5b. For comparison, activities at constant corrosion rate with and without a flow transient are also shown. The activity follows the corrosion rate curve and its slope. A linear flow rate perturbation (Eq. (10)) is also introduced at $t_0 = 500$ h. The activity in all cases eventually approaches a new saturation value. It is seen from Fig. 5(b) that the value of total specific activity due to pipe scale approaches a saturation value which depends on both the changes in flow rate (Δw) and equilibrium for corrosion rate (C_{s}). It essentially increases with increasing values of Δw approaching the constant corrosion rate values as a limit. The increase in the values of the total specific activity on pipe scale with increasing values of Δw behaves in a non-linear manner.

The behavior of coolant activity on pipe scale has also been studied for a fixed slow corrosion acceleration at

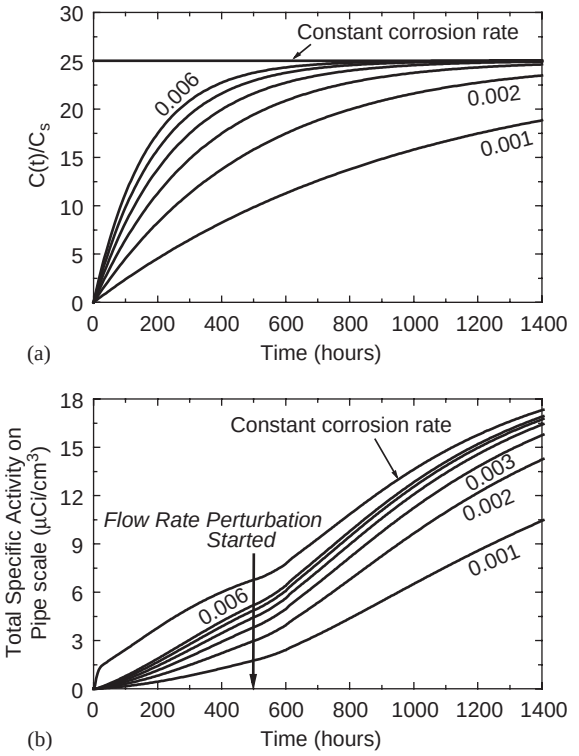

Fig. 5. (a) Normalized nonlinear corrosion rate as a function of time for various M_c values at constant equilibrium corrosion rate (C_s). (b) Total specific activity due to corrosion products on pipe scale under linear flow rate perturbation for various Δw (initiated at $t = 500$ h, $\Delta t = 100$ h) for corrosion rates shown in part (a).

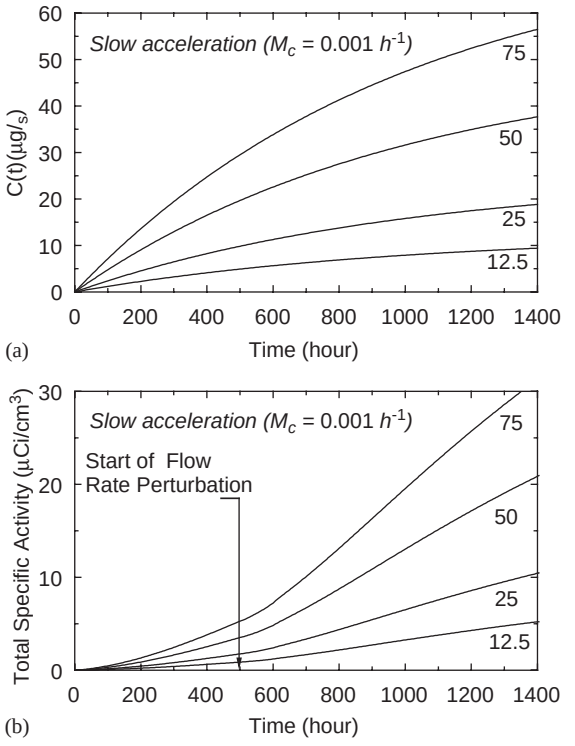

Fig. 6. (a) Slow corrosion rate as a function of time for various values of equilibrium corrosion rate (C_s) at $M_c = 0.001$/h. (b) Total specific activity due to corrosion products on pipe scale under linear flow rate perturbation for various Δw (initiated at $t = 500$ h, $\Delta t = 100$ h) for corrosion rates shown in part (a).

different equilibrium corrosion rate value (C_s from 12.5 to 75 μg/s) while the flow rate perturbation remained the same ($\Delta w = 30\%$ of w_0, initiated at $t = 500$ h for a period of 100 h). For slow acceleration in corrosion ($M_c = 0.001$/h, shown in Fig. 6a), the resulting total specific activity on pipe scale is illustrated in Fig. 6b. It is noticeable that the activity in the coolant attains new saturation value after the transient and this saturation value keeps on increasing with increase in equilibrium value (C_s). These results indicate that activity has not reached saturation after 1400 h and keeps on increasing. The saturation values are depending on both the equilibrium value of corrosion rate (C_s) and change in flow rate (Δw). However, the time taken to reach the saturation activity depends on the slope of corrosion rate. The activity depression was smeared for such a low acceleration.

Calculation for various fast corrosion acceleration models ($M_c = 0.006$/h) were also done at different equilibrium corrosion rate values. The corrosion rate and resultant activity on pipe scale are illustrated as Fig. 7a and b, respectively. The saturation values of activity change from 9.46 to 56.8 μCi/cm^3 as C_s is increased from 12.5 to 75 μg/s. The effect of flow rate just after $t = 500$ h, becomes more pronounced as the C_s value is increased beyond 25 μg/s. The tendency of activity to approach saturation also becomes apparent in these cases after 1400 h.

3.3. Effect of pump coastdown and corrosion acceleration

The primary pump coastdown due to a decrease in speed of a primary pump can be obtained by equating the frictional retarding force to the changes in the momentum of the fluid. The balance for a given average velocity (v) and fluid density (ρ) is given as (Lewis, 1977):

$$\frac{L\rho}{g_c}\frac{dv}{dt} = -C_f\frac{\rho v^2}{2g_c}, \tag{12}$$

where L is the total length of the loop and C_f is the total pressure loss coefficient for the loop. The solution in terms of flow rate is

$$w(t) = w_0/(1 + t/t_p). \tag{13}$$

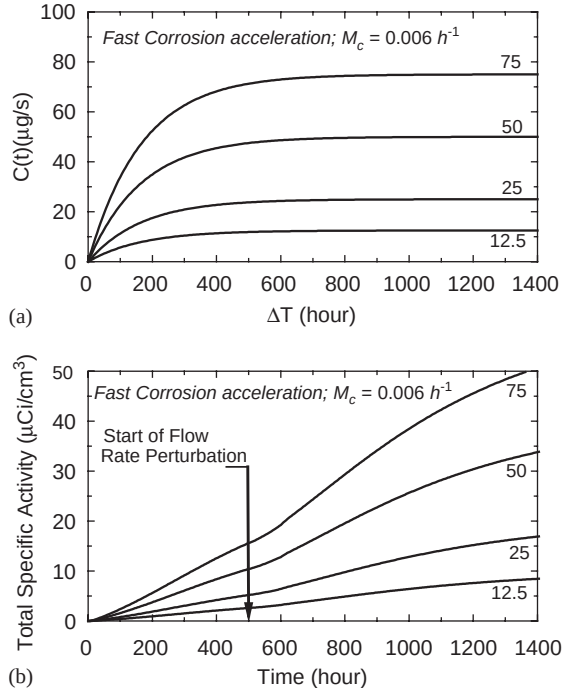

Fig. 7. (a) Fast corrosion rate as a function of time for various values of equilibrium corrosion rate (C_s) at $M_c = 0.006$/h. (b) Total specific activity due to corrosion products on pipe scale under linear flow rate perturbation for various Δw (initiated at $t = 500$ h, $\Delta t = 100$ h) for corrosion rates shown in part (a).

The time t_p is flow half-time ($2L/C_f v_0$). An initial flow rate for steady-state reactor operation is w_0 and $w(t)$ is flow rate at any time t. In this study, we considered t_p large enough (~200 h), so that the boiling crisis does not occur until after the reactor trip.

Using modified program CPAIR-P, the pump coastdown is introduced in the primary coolant circuit of a PWR for a given t_p value. Then specific activities in coolant and on pipe scale are estimated for both a constant corrosion rate and an accelerating corrosion. In this study, we allowed slope of corrosion rate to vary in steps while keeping the equilibrium value fixed at 25 μg/s. Results for primary coolant activity are shown in Fig. 8. The flow coastdown is started at $t = 1000$ h after the reactor startup until the flow rate reaches 90% of the initial flow rate value; then the reactor scrams. For a constant corrosion rate, total specific activity in the coolant approaches saturation value of 11.45 μCi/cm^3 fairly rapidly. It follows the behavior of corrosion acceleration. For a case of nonlinearly accelerated corrosion rate with a pump coastdown, the coolant activity monotonically rises and follows the slope of corrosion rate. There is a small spike due to flow coastdown after 1000 h and it becomes pronounced when nonlinear corrosion rate is fast ($M_c > 0.004$/h).

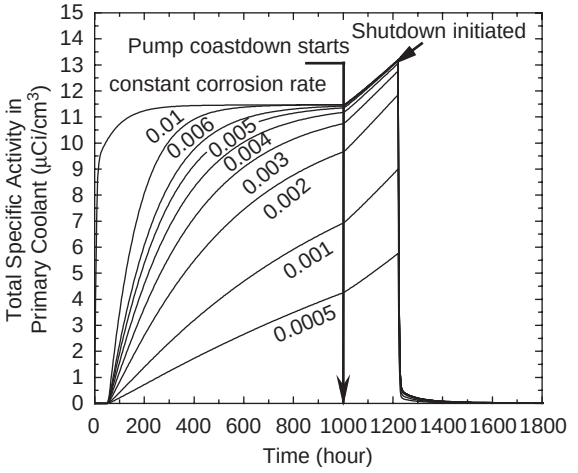

Fig. 8. Total specific activity due to corrosion products in primary coolant under pump coastdown ($t_p = 2000$ h) initiated at $t = 1000$ h for various nonlinearly rising corrosion rates at a fixed equilibrium value. Reactor scrams at 90% of its rated flow rate.

When the slope of corrosion acceleration is greater than 0.004/h then activity crosses the normal saturation value of 0.7 μCi/cm^3 before the reactor scram occurs.

Total specific activity on pipe scale for various accelerations of corrosion is shown in Fig. 9. Here corrosion rate equilibrium value was taken as 25 μg/s. Activity rises slowly and does not reach saturation value during the flow coastdown for slow acceleration in corrosion (Fig. 9). The spike is smeared and it reaches different peak values for different corrosion acceleration. The peak value and decay of activity after scram are strong functions of flow rate and efficiencies to remove activity from pipe scale.

4. Conclusions

Simulation of coolant activation due to corrosion products have been done in a typical pressurized water reactor (PWR) for nonlinearly accelerating corrosion under flow rate perturbations. In the first part of the work, the computer program CPAIR-P (Deeba et al., 1998) has been modified to accommodate for a time-dependent corrosion rate model. Results for ^{24}Na, ^{56}Mn, ^{59}Fe, ^{58}Co, ^{60}Co and ^{99}Mo show that the specific activity in primary loop approaches equilibrium value under normal operating conditions fairly rapidly. Predominant corrosion product activity during operation is due to ^{56}Mn and cobalt isotopes dominate it after shut down. Then flow rate perturbations were simulated for different corrosion rate models and their effects on saturation activity were studied. For a linear decrease in

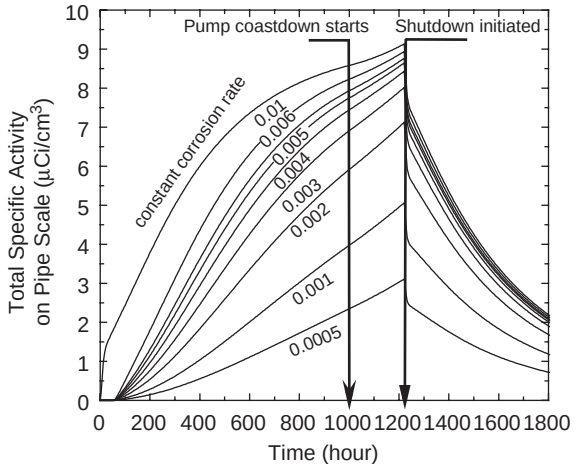

Fig. 9. Total specific activity due to corrosion products on primary pipe scale under pump coastdown ($t_p = 2000$ h) initiated at $t = 1000$ h for various nonlinearly rising corrosion rates at a fixed equilibrium value. Reactor scrams at 90% of its rated flow rate.

flow rate and a constant corrosion rate, the total coolant activity and activity on pipe scale approaches higher saturation values. For an accelerating corrosion the activities in the coolant, on core surfaces and on pipe scale attain new saturation values after the transient, and these saturation values keep on increasing with an increase in equilibrium value (C_s). These results show that the flow rate perturbations lead to a new saturation value for specific activity due to pipe scale, and the new saturation value depends on both the equilibrium value of corrosion rate (C_s) and change in flow rate (Δw). The time taken to reach the saturation activity depends on the slope of corrosion rate. For a slow pump coastdown ($t_p = 2000$ h), the activity does not show an initial drop when flow rate starts decreasing. It monotonically rises and follows the slope of corrosion rate. The peak value and decay of activity after scram are functions of flow rate and efficiencies to remove isotopes from pipe scale.

Acknowledgments

M. Rafique gratefully acknowledges the financial support of the Higher Education Commission (HEC), Pakistan, for the Ph.D. (Indigenous) fellowship under Grant # 17-6 (097) Sch/2001/4806.

References

Barry, R.F., 1963. LEOPARD: A Spectrum Dependent Non-Spatial Depletion Code for IBM-7094, WCAP-3269-26, Westinghouse Electric Corporation.

Beal, S.E., 1970. Particle deposition in turbulent flow. Nucl. Sci. Eng. 40, 1–11.

Berger, F.P., Hau, K., 1977. Mass transfer in turbulent pipe flow measured by the electrochemical method. Intl. Heat Mass Transfer 20, 1185–1194.

Bergmann, C.A., Lindsay, W.T., 1985. The role of coolant chemistry in PWR radiation field buildup, EPRI NP-4247.

Beslu, P., 1978. A computer code PACTOLE to predict activation corrosion products in PWRs. Proceedings of the International Conference on Water Chemistry of Nuclear Reactor Systems, Bournemouth, BNES, London.

Beslu, P., 1981. Mechanisim and driving forces in corrosion product transport and buildup: PACTOLE code. IAEA Specialist Meeting, San Miniato, Italy.

Cohen, P., 1969. Water coolant technology of power reactors. Gordon and Breach Sci. Publ.

Comley, G.C., 1985. The significance of corrosion products in water reactor coolant circuits. Prog. Nucl. Energy 16 (1), 41–72.

Cleaver, J.W., Yates, B., 1973. Mechanism of detachment of colloidal particles from a flat substrate in a turbulent flow. J. Coll. Interf. Sci. 44, 464–474.

Cleaver, J.W., Yates, B., 1975. A sub-layer model for the deposition of particles from a turbulent flow. Chem. Eng. Sci. 30, 983–992.

Deeba, F., Mirza, A.M., Mirza, N.M., 1999. Modeling and simulation of corrosion product activity in pressurized water reactors under power perturbations. Ann. Nucl. Energy 26 (7), 561–578.

Dey, G.R., et al., 1998. Correlation between corrosion inhibition and radiation chemical properties of some organic corrosion inhibitors. Radiat. Phys. Chem. 52 (2), 171–174.

Fontanna, M.G., 1987. Corrosion Engineering, Third ed. McGraw Hill, Singapore.

Glasstone, S., Sesonske, A., 1981. Nuclear Reactor Engineering. Von Nostradam, New York.

Hirschberg, G., Baradlai, P., Varga, K., Myburg, G., Schunk, J., Tilky, P., Stoddart, P., 1999. Accumulation of radioactive corrosion products on steel surfaces of VVER type nuclear reactors, Part I. 110 mAg. J. Nucl. Mater. 265 (3), 273–284.

Iqbal, Masood, Mirza, N.M., Mirza, S.M., Ayazuddin, S.K., 1996. Study of the void coefficients of reactivity in a typical pool type research reactor. Ann. Nucl. Energy 24 (3), 177–186 (volume date 1997).

Iqbal, Masood, Mirza, N.M., Mirza, S.M., 1998. Simulation of LEU-MTR transients under reactivity insertion and loss of flow conditions. Nucl. Sci. J. 35 (2), 81–90.

Jaeger, R.G. (Ed.), 1970. Engineering Compendium on Radiation Shielding, vol. III. Springer, New York.

Jonas, O., 2000. Effective cycle chemistry control, esaa power station chemistry. Conference Rockhampton, Queensland, Australia, May 15–16.

Kang, S., Sejvar, J., 1985. The CORA-II model of PWR corrosion product transport, EPRI NP-4246.

Khan, P., Rubina, P., Mirza, N.M., Mirza, S.M., 1999. Ramp reactivity insertion limits in a typical pool-type research reactor. Nucl. Sci. J. 36 (1), 27–41.

Lee, C.B., 1990. Modeling of corrosion product transport in PWR primary coolant. Ph.D. Thesis, Nuclear Engineering Department, MIT.

Lewis, E.E., 1977. Nuclear Power Reactor Safety. Wiley, New York.

Lister, D.H., 1976. Mass transfer in the contamination of isothermal steel surfaces. Nucl. Sci. Eng. 61, 107–118.

Lister, D.H., et al., 1985. Corrosion product release in LWRs, EPRI NP-3888.

Mandler, J.W., et al., 1985. In-Plant Source Term Measurements at Prairie Island Nuclear Generation Station, NUREG/CR-4397. US Nuclear Regulatory Commission.

Millett, P.J., Wood, C.J., 1997. Recent advances in water chemistry control at US PWRs, EPRI. Proceedings of the 58th International Water Conference, Pittsburg.

Mirza, N.M., Mirza, A.M., Qaisrani, T.M., Ahmad, N., 1989. Effect of moderator temperature on dose rate due to Na-24 at the surface of a typical swimming pool research reactor. Nucleus 263 (4), 23–28.

Mirza, N.M., Mirza, S.M., Ahmad, N., 1991. Study of coolant activation and dose rates with flow rate and power perturbations in pool-type research reactors. Nucl. Technol. 96 (3), 237–247.

Mirza, N.M., Mirza, S.M., 1993a. Assessment of orifice effects on dose rates at the reactor bridge due to coolant activation in typical MNSRs. Nucl. Energy (Br. Nucl. Energy Soc.) 32 (6), 387–394.

Mirza, N.M., Mirza, S.M., 1993b. Effects of flow rate and power perturbations on dose rates due to coolant activity in low-power research reactors. Ann. Nucl. Energy 20 (6), 381–390.

Mirza, N.M., Chughatai, S.S., Ahmad, N., Khan, L.A., 1997a. Experimental measurements of sodium-24 activity in a typical low power tank-in-pool type research reactor. Nucl. Sci. J. 34 (3), 203–208.

Mirza, A.M., Mirza, N.M., Mir, I., 1997b. Simulation of corrosion product activity in pressurized water reactors under flow rate transients. Ann. Nucl. Energy 25 (6), 331–345 (volume date 1998).

Mirza, A.M., Khanam, S., Mirza, N.M., 1998. Simulation of reactivity transients in current MTRs. Ann. Nucl. Energy 25 (18), 1465–1484.

Morillon, A., 1987. Modelling of radionuclide transport in a simulated PWR environment. M.S. Thesis, Nuclear Engineering Deptartment, MIT.

Nasir, R., Mirza, N.M., Mirza, S.M., 1999. Sensitivity of reactivity insertion limits with respect to safety parameters in a typical MTR. Ann. Nucl. Energy 26 (17), 1517–1535.

Moore, T., 1984. Robots join the nuclear work force. EPRI J.

Oelkers, E.H., Helgeson, H.C., 1988. Calculation of the thermodynamic and transport properties of aequeous species at high pressure and temperature. Geochim. et cosmoch. Acta 52, 63–85.

Polley, M., Pick, M., 1986. Iron, nickel and chromium mass balances in Westinghouse PWR primary circuits. Proceedings of the International Conference on Water Chemistry of Nuclear Systems, Bournemouth, 4 BNES, London.

Raymond, A., De Murcia, A., Dhaunut, S., 1987. Speciation and analysis of corrosion products in the primary coolant of pressurized water reactors. Anal. Chim. Acta 195, 265–273.

Strasser, A., et al., 1985. Corrosion product buildup on LWR fuel rods. EPRI NP-3789.

Sanchez, R., 1989. Use of a pressurized in-pile loop ro reduce dose rates by improving PWR coolant chemistry. Ph.D. Thesis, Nuclear Engineering Department, MIT.

Thomas, J.R., Edlund, H.C., 1980. Reactor statics module—multi-group criticality calculations. Proceedings of the Conferenc on ICTP, Trieste.

Varga, K., Hirchberg, G., Nemth, Z., Myburg, G., Schunk, J., Tilky, P., 2001. Accumulation of radioactive corrosion products on steel surfaces of VVER-type nuclear reactors. II. ^{60}Co. J. Nucl. Mater. 298 (3), 231–238.

Volleque, P.G., 1990. Measurements of radioiodine species in samples of pressurized water coolant. Nucl. Technol. 90, 23–33.